PROMETHEUS PRESS/PALAEONTOLOGICAL NETWORK FOUNDATION (TERUEL)

Journal of Taphonomy

2017 *Available online at www.journaltaphonomy.com*

VOLUME 15 (ISSUE 1-3)

First Steps into the Microscopic Metrical Characterization of Bone Weathering in a Sample of Modern Guanaco (*Lama guanicoe*) from Southern Patagonia, Argentina: Implications for Patterns of Intraosseous Differential Preservation

Natalia Morales*, Gustavo Barrientos

División de Arqueología/División de Antropología, Facultad de Ciencias Naturales y Museo
Universidad Nacional de La Plata, Paseo del Bosque s/n. (1900), La Plata, Buenos Aires, Argentina
CEAR, Facultad de Humanidades y Artes, Universidad Nacional de Rosario
Entre Ríos 758, (2000), Rosario, Santa Fe, Argentina

Juan Bautista Belardi

Universidad Nacional de la Patagonia Austral (ICASUR, CONICET)
Campus Universitario Avda. Gregores y Piloto Lero Rivera s/n. (9400)
Río Gallegos, Santa Cruz, Argentina

Journal of Taphonomy 15 (1-3) (2017), 109-122.
Manuscript received 3 June 2017, revised manuscript accepted 4 September 2017.

In many southern Patagonia archaeological bone assemblages deposited in open-air settings, a remarkable difference in preservation between shafts and epiphyses of guanaco (*Lama guanicoe*) long bones, leading to an overrepresentation of the latter, has been found. It has been suggested that, in dynamic sedimentary deposits like those investigated in this region, the observed pattern is mainly related to subaerial weathering or to a combination of weathering and abrasion preferentially affecting long bone shafts, processes that may have little relationship with bone mineral density (BMD). In order to investigate in more detail the relationship between weathering and bone mineral density (BMD) and cortical thickness in guanaco long bones, a microscopic (low magnification) metrical analysis of partial cross-sections from a sample of modern radii-ulnae with a various degrees of weathering was performed. Overall, the obtained results suggest that subaerial weathering can suffice to explain the observed archaeological pattern of differential intraosseous preservation, although this inference should be further supported with data from a larger sample including other long bones as well as a more complete record of the weathering sequence.

Keywords: PATAGONIA, *LAMA GUANICOE*, LONG BONES, DIFFERENTIAL INTRAOSSEOUS PRESERVATION, WEATHERING.

*E-mail: moralesnatalia@fcnym.unlp.edu.ar

Introduction

In southern Patagonia, particularly in the Cardiel and Tar lake basins (Santa Cruz, Argentina) (Figure 1), a remarkable difference in preservation between shafts and proximal and distal ends (epiphysis plus metaphysis) of guanaco (*Lama guanicoe*) long bones has been found in Late Holocene archaeological bone assemblages deposited in open-air settings situated at different altitudes above sea level, and in both clayey and sandy sediments (Belardi *et al.*, 2010, 2012; Rindel & Bourlot, 2014). Contrary to the expectations derived from the knowledge about density-mediated processes of bone destruction like carnivore gnawing, some human culinary practices, and subsurface degradation (*e.g.*, Guthrie, 1967; Brain, 1969; Marean & Kim, 1998; Pickering *et al.*, 2003; Faith & Behrensmeyer, 2006; Faith *et al.*, 2007; Yravedra & Domínguez-Rodrigo, 2009; Madgwick & Mulville, 2012), in the study region proximal and distal ends tend to be overrepresented in bone assemblages recovered primarily from sites situated at the eastern and southern shores of the Cardiel Lake and at the eastern shore of Tar Lake (Figure 1). It has been proposed that, in dynamic sedimentary deposits like those investigated in this region, in which bones can be alternatively exposed or buried, the observed pattern is mainly related to subaerial weathering or to a combination of weathering and abrasion preferentially affecting long bone shafts (Belardi *et al.*, 2010, 2012), processes that may have little relationship with bone mineral density (BMD) (Lam *et al.*, 1999; Ioannidou, 2003; Madgwick & Mulville, 2012; Fernández-Jalvo & Andrews, 2016). Due to this fact, the correlation between some measure of bone survivorship (*e.g.*, MNE, MAU, %MAU, %survivorship; Lyman, 1994) and BMD would be an

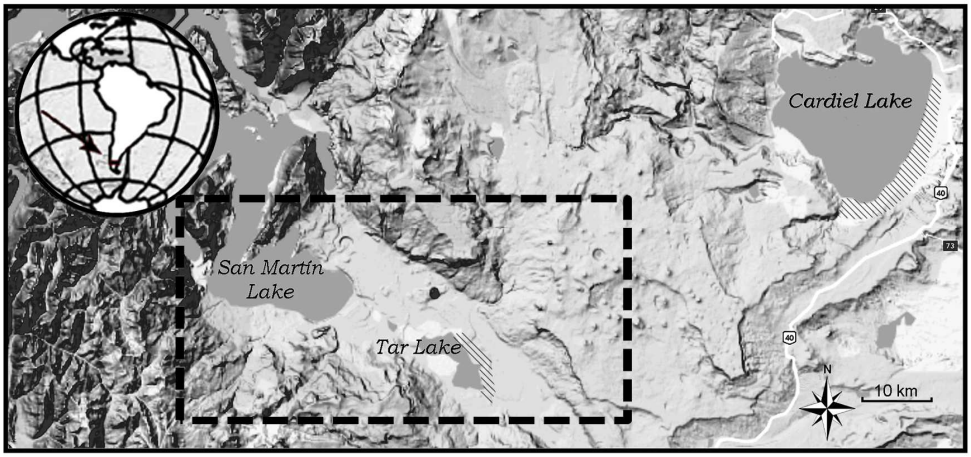

Figure 1. Portion of southern Patagonia from where the archaeological observations referred in the text were made; the dashed area east and south of Cardiel Lake and east of Tar Lake represent the distribution of the archaeological sites where the pattern of differential preservation of epiphyses and diaphysis in guanaco long bones was observed; enclosed within the dashed lines is the area from where the modern guanaco bone sample was collected.

inadequate or partial tool to evaluate and interpret the integrity of archaeofaunas from many southern Patagonia open-air sites (and, potentially, from other similar environments).

Subaerial weathering is the result of a combination of physical and chemical processes leading to the progressive separation and destruction of the original microscopic organic and inorganic components of bone (Behrensmeyer, 1978:153). It manifests as a succession of changes involving surface cracking, flaking, exfoliation, splitting and, ultimately, disintegration of bone elements (Behrensmeyer, 1978; Steele & Carson, 1989; Fisher, 1995). Several observational and experimental studies have analyzed both the way in which the weathering process affects the bones of large and small vertebrates under different environmental conditions (*e.g.*, Miller, 1975; Behrensmeyer, 1978; Andrews, 1990, 1995). It has been observed that weathering follows a general pattern of progression, although with remarkable differences in rate at many relevant levels, for example taxonomic (Gifford, 1981; Gutiérrez *et al.*, 2016), age group (Behrensmeyer, 1978; Massigoge *et al.*, 2010; González *et al.*, 2012; Gutiérrez *et al.*, 2016), anatomical (Behrensmeyer, 1978; Gifford, 1981; Todd *et al.*, 1987; Lyman & Fox, 1989; Madgwick & Mulville, 2012). Other factors affecting the rate of subaerial weathering are the micro and macroenvironmental conditions under which carcasses or isolated bone elements are deposited (*i.e.*, substrate, climate, etc.; Behrensmeyer, 1978; Andrews & Cook, 1985; Ubelaker & Sperber, 1988; Fiorillo, 1989; Tappen, 1994; Beary, 2005; Potmesil, 2005; Conard *et al.*, 2008; Janjua & Rogers, 2008; Miller, 2009; Pokines, 2009; Pokines *et al.*, 2011, 2016; Madgwick & Mulville, 2012; Junod 2013; Junod & Pokines, 2014).

In order to investigate in more detail the relationship between weathering, BMD, and cortical thickness in guanaco long bones, we continued a transactional study of modern carcasses initiated early this decade (Belardi *et al.*, 2010, 2012). In this paper we present the first results of an exploratory microscopic (low magnification) metrical analysis of partial cross-sections from a sample of modern guanaco long bones (radii-ulnae) with a various degree of weathering recovered along several field seasons at open-air settings in the Tar and San Martín lake basins. The specific aim of this research is to describe the sequence of macroscopic and microscopic changes of bone tissues related to subaerial weathering at definite anatomical locations whose mean BMD values are known (Stahl, 1999). The relevance of this study for the zooarchaeological and taphonomic discussion in this region is related to the major importance that guanacos —large social ungulates weighting around 100 kg— had for past Patagonian hunter-gatherer economy (Borrero, 1990; Miotti, 1998; Mengoni Goñalons, 1999; Belardi *et al.*, 2017). The environmental characteristics of the study area and several other details of the research problem were extensively described in a paper already published in this journal (Belardi *et al.*, 2012), so they will not be addressed here.

Materials and methods

The analyzed sample was composed of ten radii-ulnae corresponding to ten different modern adult guanaco carcasses (sex: undetermined; time since death: unknown) with a various degree of skeletonization and weathering, recovered along several field

seasons at different open-air settings in the Tar and San Martín lake basins (Belardi *et al.*, 2012) (Figure 1). Table 1 describes the preservation state of each sampled element. At four locations on the bone surface, corresponding to the scan sites RU1, RU4, RU5 and RU6 defined by Stahl (1999) in his study of South American camelids bone mineral density, a weathering stage on the six-point (0 to 5) scale developed by Behrensmeyer (1978) was recorded. Generic camelid (*Lama*) BMD data from Stahl (1999) were used over the specific guanaco BMD data from Elkin and Zanchetta (1991) for the simple reason that the former uses more scan sites per skeletal element with a more precise description of its localization (Izeta, 2005:1161, Table 1).

In order to model the spatial variations in bone weathering along the surface of each specimen, data from the four scan sites were interpolated using kriging in the free and open source GIS package QGIS 2.14.3, assuming that weathering actually varies continuously along a single bone element. The resulting model was then used to evaluate the degree to which the suite of sampled specimens constitutes a complete representation of the weathering continuum.

At the above mentioned scan sites, an anterior hemi cross-section of bone (≈5 mm) was extracted with the aid of a hand-held mini drilling machine provided with a cutting wheel. The proximal cut surface of each specimen was observed under incident light with a stereomicroscope (magnification range of 10x to 40x). Under the microscope and with the aid of an electronic caliper (0-150 mm/0.01 mm), seven metric variables characterizing the morphology of surface and inner cracks, both longitudinal and concentric, were measured (Figure 2):

A) Maximum crack depth (MCD): depth of the deepest crack;

B) Crack breadth (CB): surface breadth of the deepest crack;

C) Crack continuation (CC): distal prolongation of the deepest crack not presenting noticeable separation of bone tissues at the time of measurement;

D) Cortical bone thickness (CBT): cortical thickness at the place where the MCD was measured; in cases in which no fissure was present, the measurement was conventionally taken at the mid-point of the hemi cross-section;

E) Lateral crack length (LCL_1-LCL_1'… LCL_n-LCL_n'): length of the concentric cracks lateral to the deepest longitudinal crack (right and left side, respectively);

F) Lateral crack depth at the origin (LCD_{1a}-LCD_{1a}'…LCD_{na}-LCD_{na}'): vertical distance between the origin of each lateral crack and the bone cortical surface (right and left side, respectively);

G) Lateral crack depth at the end (LCD_{1b} -LCD_{1b}'…LCD_{nb}-LCD_{nb}'): vertical distance between the end of each lateral crack and the bone cortical surface (right and left side, respectively).

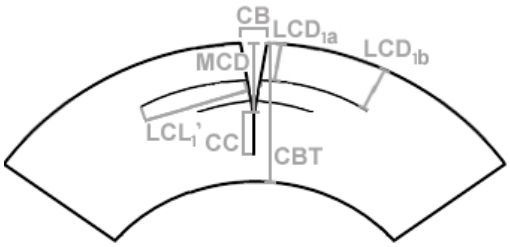

Figure 2. Metric variables recorded in each hemi cross-section of bone (radius-ulna) (see text for the description of each variable).

Table 1. Description of the preservation state of each modern guanaco radius-ulna specimen analyzed.

Specimen	Laterality	Observations
SP1	right	Soft tissues attached to bone surfaces in both ends and on the shaft; bone marrow in the interior of medullary canal and in both ends of the bone.
SP2	right	Soft tissues attached to bone surfaces in both ends of the bone; greenish spot on the distal side of the bone.
SP3	right	Soft tissues attached to bone surfaces in both ends of the bone; insect pupae in the medullary cavity; black dots on the surface.
SP4	left	Greenish and black spots in the cancellous bone.
SP5	left	Black dots on the surface; greenish and orange spots in the cancellous bone.
SP6	left	Black dots on the surface; greenish and orange spots in the cancellous bone; chunks of trabecular bone and indurated sediment in the medullary canal.
SP7	right	Black and greenish spots in both compact and cancellous bone; chunks of trabecular bone and non-indurated sediment in the medullary canal.
SP8	left	Black dots on the surface; greenish spots in the cancellous bone; sand in the medullary canal.
SP9	right	Black dots on the surface; greenish spots in the cancellous bone; vegetal remains (leaves) in the medullary canal.
SP10	left	Greenish spots in the cancellous bone; sand in the medullary canal.

Basic descriptive statistics for the different metric variables were computed as well as a suite of nonparametric test (Spearman rank order correlation and Kolmogorov-Smirnov two-sample test).

Results

Figure 3 illustrates that there seems to be no direct relationship between weathering and bone mineral density; in effect, portions of

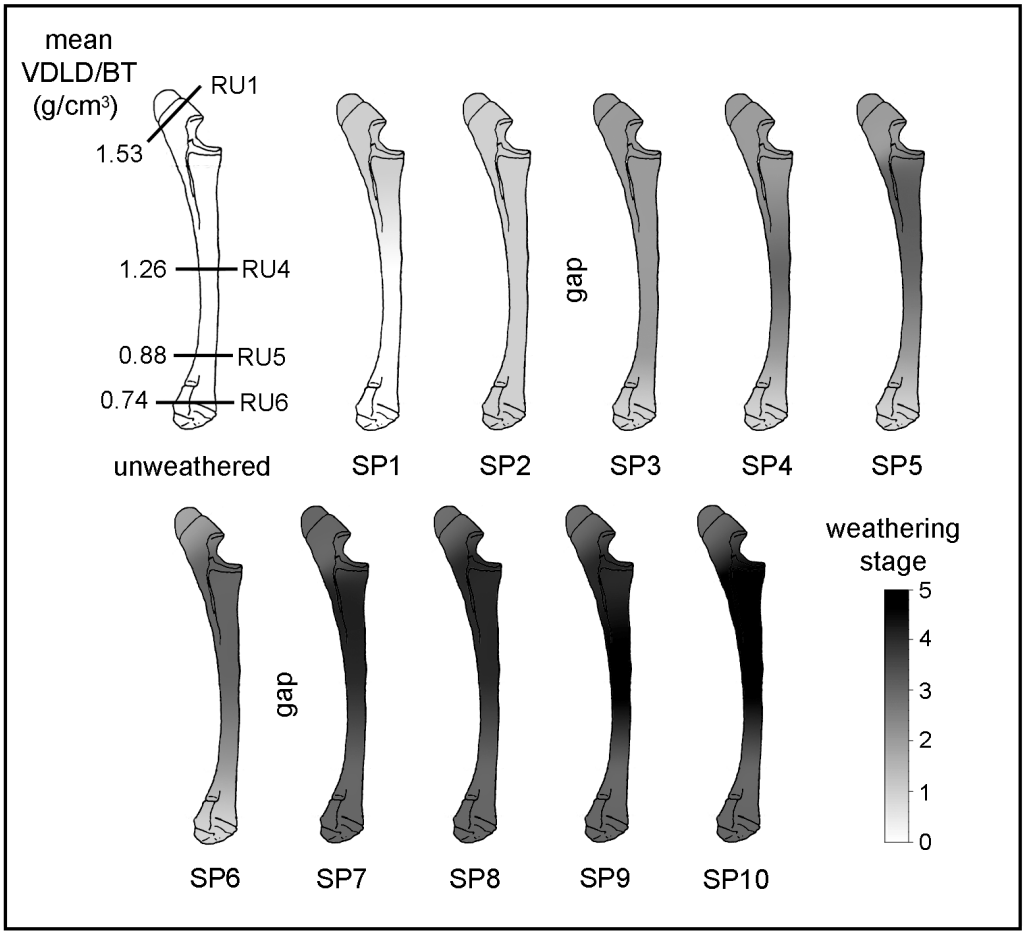

Figure 3. Modern guanaco radius-ulna specimens ordered in a progressive weathering sequence modelled using kriging. The two inferred gaps in the sequence are indicated. In the left upper row, an ideal unweathered specimen is represented showing the anatomical distribution of the scan sites considered as well as their corresponding bone mineral density values [VDLD/BT (g/cm^3); Stahl (1999)].

the bone with quite different values of BMD [VDLD/BT (g/cm^3); (Stahl, 1999)] react in a very similar way to subaerial weathering agents (*e.g.*, proximal and distal ends of the bone, midshaft and distal segment of the shaft) and, at the same time, portions with relatively close values of BMD weather at different rates (*e.g.*, proximal epiphysis and midshaft segment of the bone). Figure 3 also illustrates that at least two major gaps in the sequence of weathering can be identified at the total sample level: the first one between specimens 2 and 3, and the second one —the most significant— between specimens 6 and 7. Despite the latter fact, it can be said that the analyzed sample describes fairly well the progression of weathering across the radius-ulna. In particular it is interesting to note that the general pattern seems to be one in which the midshaft —particularly its upper portion— is about two stages ahead of the proximal and distal ends of the bone (epiphyses and proximal and distal quarters of the shaft), at least from the stage represented by specimen 3 onwards. Figure 3 also clearly illustrates that while both ends of the bone remain in stage 3, the shaft progresses to stage 5, with an evident destruction of the element.

In Table 2 the values of the quantitative variables measured in each hemi cross-section (expressed in mm) are shown. With the exception of two cases —SP10-RU1 and SP10-RU4, in which the preservation state of the samples due to weathering (stage 5) made impossible the observations— all variables, when the described feature was present, could be measured. Lateral cracks were only present in the cortical bone of the shaft, particularly at the scan site RU4.

Figure 4 shows the distribution of CBT values for the hemi cross-sections corresponding to each Stahl's scan sites. In RU4 and RU5, the median values of CBT are about 4 and 6 times greater than in RU1 and RU6.

With the sole exception of specimen 1, all elements have cracks or fissures of different size affecting both cortical and cancellous bone. The correlation between MCD and CB is high and statistically significant at an alpha level of 0.01 only for RU1 and RU6 (Spearman Rho=0.92 and 0.85, respectively). In the case of the shaft, the correlation between both variables is moderate (RU4) or very low (RU5) so the width of the crack cannot be considered, in this particular portion of the bone, a good predictor of its depth.

Figures 5 and 6 are representations of the relationship between the weathering stage and the ratio between MCD and CBT for the shaft and bone ends, respectively. In the proximal and distal ends, the MCD/CBT ratio reaches a value of 1 (*i.e.*, the crack runs through the entire thickness of the cortical bone) at weathering stage 1 (RU1) or 2 (RU6). In weathering stage 3 —the maximum stage recorded— all hemi cross-sections have fissures that penetrate well into the cancellous bone (indicated by MCD/CBT ratio values higher than 1). In the shaft, longitudinal cracks do not penetrate more than 20% of the cortical bone until stage 3 (Figure 7); at this stage there is a variable degree of penetration, reaching in many cases (SP4-RU4, SP8-RU5, SP9-RU5, SP10-RU5) 100% of the cortical bone (*i.e.*, MCD/CBT ratio=1).

The total number of lateral cracks recorded in this sample is low (n=7), being present only in the shaft. This kind of cracks seems to appear only when the MCD/CBT ratio is equal to 1 in weathering stage 3 or higher, but not all cracks that run throughout the entire cortical bone have lateral cracks (*e.g.*, in SP7-RU4, SP8-RU5, and SP10-RU5).

Sample	WS	MCD	CB	CC	CBT	LCL_1	LCD_{1a}	LCD_{1b}	LCL_2	LCD_{2a}	LCD_{2b}	LCL_1'	LCD_{1a}'	LCD_{2b}'
SP1-RU1	1	0.00	0.00	0.00	0.48	-	-	-	-	-	-	-	-	-
SP1-RU4	0	0.00	0.00	0.00	8.33	-	-	-	-	-	-	-	-	-
SP1-RU5	0	0.00	0.00	0.00	5.14	-	-	-	-	-	-	-	-	-
SP1-RU6	0	0.00	0.00	0.00	1.65	-	-	-	-	-	-	-	-	-
SP2-RU1	1	0.11	0.13	0.00	0.48	-	-	-	-	-	-	-	-	-
SP2-RU4	1	0.95	0.21	1.07	5.12	-	-	-	-	-	-	4.18	2.29	2.36
SP2-RU5	1	0.45	0.44	1.35	4.84	-	-	-	-	-	-	-	-	-
SP2-RU6	1	0.59	0.23	0.84	1.44	-	-	-	-	-	-	-	-	-
SP3-RU1	2	0.45	0.28	0.20	0.51	-	-	-	-	-	-	-	-	-
SP3-RU4	2	0.26	0.35	0.00	4.30	-	-	-	-	-	-	-	-	-
SP3-RU5	2	0.36	0.59	0.00	4.01	-	-	-	-	-	-	-	-	-
SP3-RU6	1	0.32	0.25	1.47	0.33	-	-	-	-	-	-	-	-	-
SP4-RU1	2	0.18	0.12	0.00	0.64	-	-	-	-	-	-	-	-	-
SP4-RU4	3	6.11	0.93	0.00	6.11	5.69	2.95	1.08	-	-	-	-	-	-
SP4-RU5	2	0.40	0.25	0.80	5.03	-	-	-	-	-	-	-	-	-
SP4-RU6	1	0.27	0.09	0.00	1.81	-	-	-	-	-	-	-	-	-
SP5-RU1	2	0.53	0.32	0.00	0.58	-	-	-	-	-	-	-	-	-
SP5-RU4	3	0.19	0.36	0.00	5.80	-	-	-	-	-	-	-	-	-
SP5-RU5	2	0.31	0.21	0.00	3.75	-	-	-	-	-	-	-	-	-
SP5-RU6	1	1.00	0.18	0.25	1.45	-	-	-	-	-	-	-	-	-
SP6-RU1	2	0.50	0.24	0.16	0.50	-	-	-	-	-	-	-	-	-
SP6-RU4	3	1.19	0.31	1.53	6.26	-	-	-	-	-	-	-	-	-
SP6-RU5	2	0.56	0.12	0.00	5.21	-	-	-	-	-	-	-	-	-
SP6-RU6	1	0.45	0.06	1.68	0.63	-	-	-	-	-	-	-	-	-
SP7-RU1	3	1.09	0.62	0.00	0.25	-	-	-	-	-	-	-	-	-
SP7-RU4	4	5.15	2.55	0.00	5.15	-	-	-	-	-	-	-	-	-
SP7-RU5	3	1.04	0.39	1.02	3.70	-	-	-	-	-	-	-	-	-
SP7-RU6	3	1.38	0.44	0.00	0.00	-	-	-	-	-	-	-	-	-
SP8-RU1	3	1.22	0.43	0.00	0.00	-	-	-	-	-	-	-	-	-
SP8-RU4	4	4.07	0.54	0.00	4.07	2.58	1.93	1.49	-	-	-	-	-	-
SP8-RU5	3	3.81	0.47	0.00	3.81	-	-	-	-	-	-	-	-	-
SP8-RU6	3	2.45	0.62	0.00	0.80	-	-	-	-	-	-	-	-	-
SP9-RU1	3	0.79	0.44	0.00	0.32	-	-	-	-	-	-	-	-	-
SP9-RU4	5	6.35	0.78	0.00	6.35	2.11	1.72	2.78	1.95	4.06	3.91	2.22	2.70	1.94
SP9-RU5	3	5.61	0.16	0.00	5.61	-	-	-	-	-	-	2.70	2.24	0.00
SP9-RU6	3	1.24	0.25	0.00	0.45	-	-	-	-	-	-	-	-	-
SP10-RU1	3	ns	ns	ns	ns	ns	ns	ns	ns	ns	ns	ns	ns	ns
SP10-RU4	5	ns	ns	ns	ns	ns	ns	ns	ns	ns	ns	ns	ns	ns
SP10-RU5	3	2.91	1.86	0.00	2.91	-	-	-	-	-	-	-	-	-
SP10-RU6	3	1.13	0.39	0.00	0.24	-	-	-	-	-	-	-	-	-

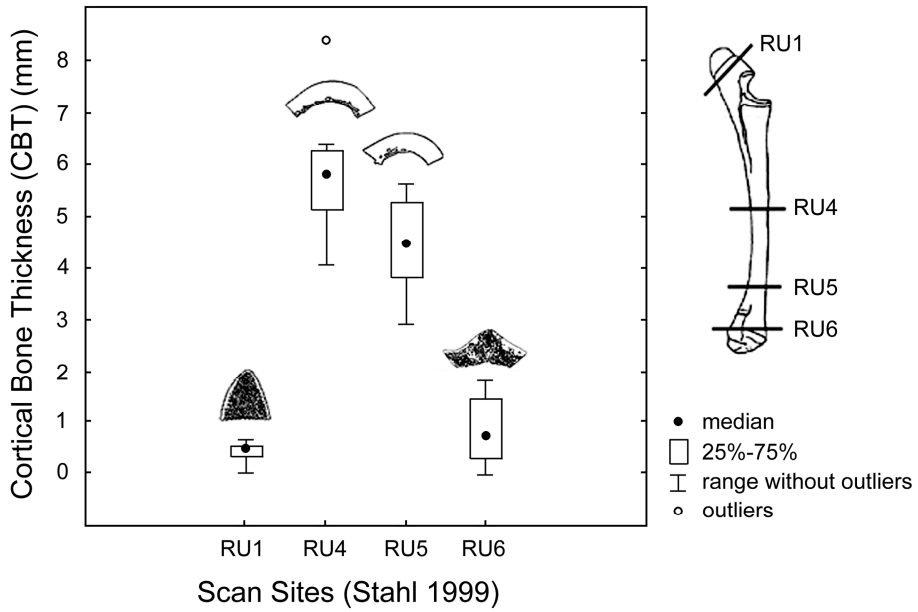

Figure 4. Box-and-whiskers plots showing the distribution of cortical bone thickness (CBT) values measured in modern guanaco radius-ulna specimens at each of the four scan sites (Stahl 1999) considered in this study. Above each box-and-whiskers plot, the morphology of the corresponding cross sections is represented.

There is no clear relationship between the depths at the origin and at the end of each fissure and the corresponding crack length (Spearman Rho=0.04 and -0.71, statistically non-significant at an alpha level of 0.01). The trajectory of the lateral cracks is generally ascendant (5/7 or 71%), although there are not statistically significant differences between the depth at the origin and at the end of the detected cracks globally (Kolmogorov-Smirnov two-sample test at an alpha level of 0.01).

Discussion

Regarding the progression of weathering along the bone, our data indicate that cortical bone tissue behaves differently across the shaft: weathering tends to spread, from stage 2 onwards, from approximately the centre of the shaft to its upper half; as the process advances, the portion near the distal metaphysis remains in stage 3, even though the upper half of the shaft reaches stage 5. This pattern has been observed in

Table 2 (previous page). Metric dataset. References: Weathering stage (WS); Maximum crack depth (MCD); Crack breadth (CB); Crack continuation (CC); Cortical bone thickness (CBT); Lateral crack length (LCL); Lateral crack depth at the origin (LCD_{1a}); Lateral crack depth at the end (LCD_{1b}).

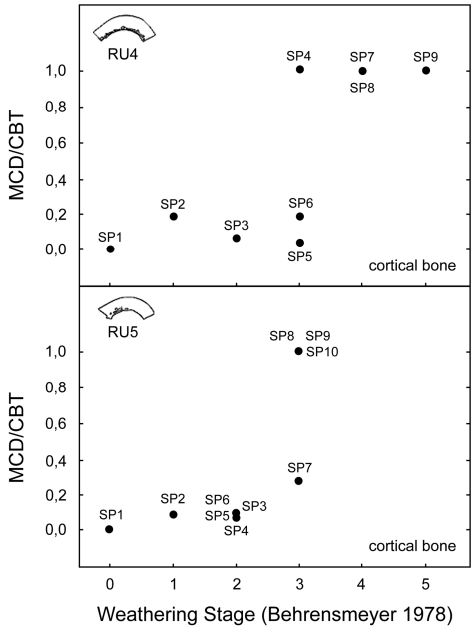

Figure 5. Scatter plot of the relationship between weathering and the maximum crack depth/cortical bone thickness ratio (MCD/CBT) for diaphyseal scan sites (RU4 and RU5; Stahl 1999).

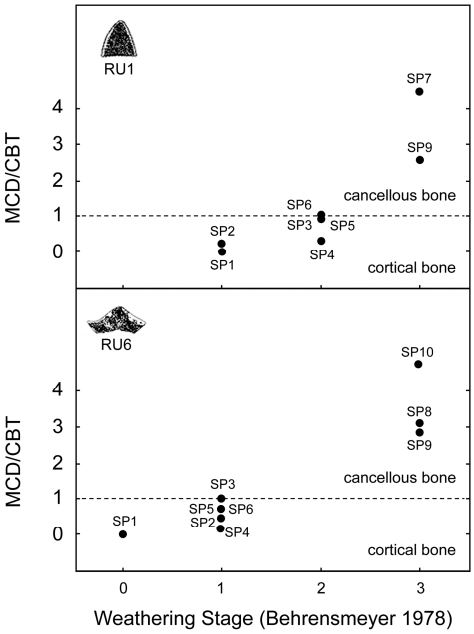

Figure 6. Scatter plot of the relationship between weathering and the maximum crack depth/cortical bone thickness ratio (MCD/CBT) for epiphyseal scan sites (RU1 and RU6; Stahl 1999). In both cases, the dashed line represents the boundary (MCD/CBT=1) between cortical (below) and cancellous (above) bone.

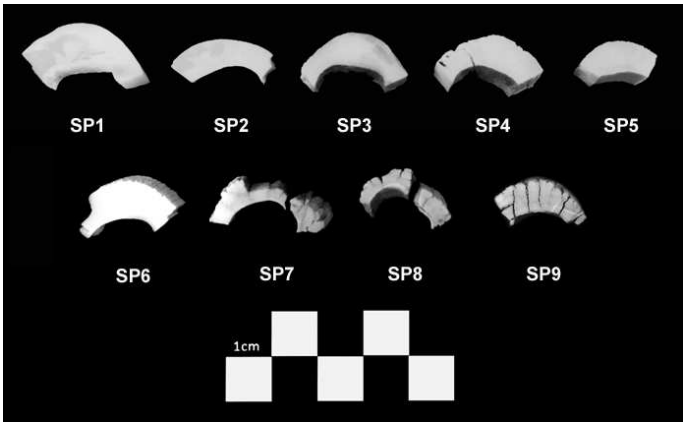

Figure 7. Proximal surface of sampled hemi cross-sections of bone at the Stahl's (1999) RU4 scan site (specimens 1 to 9).

different guanaco long bones in the study area coming from both archaeological and modern assemblages.

At the midshaft, near-concentric internal cracks —lateral to the main longitudinal cracks— begin to form at stage 3 and are invariably present at higher stages. The formation of this kind of internal cracking pattern is delayed, when present, in the distal third of the shaft. This kind of inner cracks was recorded in experimental studies of freeze-thaw cycles (Miller, 1975; Guadelli, 2015; Pokines *et al.*, 2016). It has been observed that the water frozen inside the pores and fissures of the bone has a high potential to further contribute to the cracking caused by weathering (Matsuoka, 1996; Guadelli, 2008, 2015; Pokines *et al.*, 2016). Because the bones analyzed in this research were obtained from soil surfaces that are covered by snow in winter, the presence of lateral cracks could be likely due to repeated cycles of freezing and thawing.

In our sample, as the weathering of the middle and proximal part of the shaft progresses, the proximal and distal epiphyses of the bone remain virtually unchanged (staying in stage 3). As a technical note, it can be said that the apparent quiescence of the ends of the bone, particularly of the epiphyses, in weathering stage 3 while other portions progress to higher stages may in fact be an artifact derived from the use of Behrensmeyer's scale beyond its proper limits, since it has not been specifically designed to assess weathering at the epiphyses. It is important to remember that such scale is designed only to describe changes in compact or cortical bone, preferably in the diaphysis of long bones, flat surfaces of jaws, pelvis, vertebrae, and ribs (Behrensmeyer, 1978:152; see also Lyman, 1994:358). Structural changes in the epiphyses attributable to weathering seemingly consist —once the thin cortical layer has been removed— of the progressive deepening of fissures or cracks. Other associated modifications like the erosion of cancellous bone, with the consequent loss of volume (Cunningham *et al.*, 2011), can be considered the effects of bone weakened by weathering being susceptible to trampling or other kinds of postmortem damage.

Beyond this, it is clear that rates of tissue destruction attributable to weathering are different in shaft and bone ends, which would explain the observations made by Belardi *et al.* (2010, 2012) at different open-air sites. In any case, a deeper understanding of the differential patterns of diaphysis and epiphysis weathering depends on the development of macroscopic and microscopic descriptive criteria specific to the sequence of changes, as well as the possibility to relate such changes to intraosseous variations in the structure and mechanical properties of cortical and cancellous bone tissues (*e.g.*, Riggs *et al.*, 1993; Endo *et al.*, 2016).

Conclusions

Although the results obtained in this study seem to indicate that recurrent patterns of differential bone preservation found in assemblages recovered at open-air settings in southern Patagonia were likely caused by weathering, this inference should be further supported with data from a bigger sample including other long bones as well as a more complete record of the weathering sequence.

Although subaerial weathering can suffice to explain the observed archaeological pattern of differential intraosseous preservation, an aspect that

should be addressed in the future is the role of abrasion and its combined effects with weathering (Belardi *et al.*, 2010, 2012), since it has been demonstrated that abrasion can be a major destructive force in sandy and stony environments like dunes and gravels (Behrensmeyer, 1990, 1991; Fernández-Jalvo, 1992; Andrews, 1995; Fernández-Jalvo & Andrews, 2003, 2016), which are common geologic deposits in the study area.

Acknowledgements

We want to express our gratitude to María Clara Álvarez and Daniela Alunni for their kind invitation to contribute to this volume and to two anonymous reviewers for their valuable comments and suggestions. This research was funded by grants from UNPA (PIP 29/A304 and PIP 29/A360-1) and CONICET (PIP-0622).

References

Andrews, P. (1990). *Owls, Caves and Fossils*. Natural History Museum and University of Chicago Press, Chicago.

Andrews, P. (1995). Experiments in taphonomy. *Journal of Archaeological Science,* 22: 147-153.

Andrews, P. & Cook, J. (1985). Natural modifications to bones in a temperate setting. *Man,* 20: 675-691.

Beary, M.O. (2005). *Estimation of Bone Exposure Duration Through the Use of Spectrophotometric Analysis of Surface Bleaching and its Application in Forensic Taphonomy*. Mercyhurst University, Erie.

Behrensmeyer, A.K. (1978). Taphonomic and ecological information from bone weathering. *Paleobiology*, 4 (2): 150-162.

Behrensmeyer, A.K. (1990). Bones. In (Briggs, D.E. G. & Crowther, P.R., eds.) *Palaeobiology: a Synthesis*. Blackwell Scientific, Oxford, pp. 232-235.

Behrensmeyer, A.K. (1991). Terrestrial vertebrate accumulations. In (Allison P.A. & Briggs, D.E.G., eds.) *Taphonomy: Releasing the Data Locked in the Fossil Record.* New York: Plenum Press, pp. 291-335.

Belardi, J.B., Bourlot, T. & Rindel, D. (2010). Representación diferencial de diáfisis y epífisis de huesos largos de guanaco (*Lama guanicoe*) en contextos arqueológicos de médanos en Patagonia austral: el sitio Río Meseta 1 (lago Tar, provincia de Santa Cruz). In (Gutiérrez, M.A., De Nigris, M., Fernández, P.M., Giardina, M., Gil, A., Izeta, A., Neme, G. & Yacobaccio, H., eds.) *Zooarqueología a Principios del Siglo XXI. Aportes Teóricos, Metodológicos y Casos de Estudio*. Buenos Aires: Ediciones del Espinillo, pp. 119-131.

Belardi, J.B., Rindel, D. & Bourlot, T. (2012). Much more than it was expected: preservational differences of diaphysis and epiphyseal ends of guanaco (*Lama guanicoe*) long bones in southern Patagonia (Argentina). *Journal of Taphonomy,* 10 (1): 45-65.

Belardi, J.B., Carballo Marina, F., Madrid, P., Barrientos, G. & Campan, P. (2017). Late Holocene guanaco hunting grounds in southern Patagonia: blinds, tactics and differential landscape use. *Antiquity,* 91 (357): 718-731.

Borrero, L.A. (1990). Fuego-Patagonian bone assemblages and the problem of communal guanaco hunting. In (Davis, L. & Reeves, B.O.K., eds.) *Hunters of the Recent Past.* London: Unwin Hyman, pp. 373-399.

Brain, C.K. (1969). The contribution of the Namib Desert Hottentots to and understanding of Australopithecine bone accumulations. *Scientifc Papers of the Namib Desert Research Station,* 39: 13-22.

Conard, N.J., Walker, S.J. & Kindle, A.W. (2008). How heating and cooling and wetting and drying can destroy dense faunal elements and lead to differential preservation. *Palaeogeography, Palaeoclimatology, Palaeoecology,* 266: 236-245.

Cunningham, S.L., Kirkland, S.A. & Ross, A.H. (2011). Bone weathering of juvenile-sized remains in the North Carolina piedmont. In (Ross, A.H. & Abel, S.M., eds.) *The Juvenile Skeleton in Forensic Abuse Investigations.* New York: Springer, pp.179-196.

Elkin, D.C. & Zanchetta, J.R. (1991). Densitometría ósea de camélidos. Aplicaciones arqueológicas. *Shincal*, 3: 195-204.

Endo, K., Yamada, S., Todoh, M., Takahata, M., Iwasaki, N. & Tadano, S. (2016). Structural strength of cancellous specimens from bovine femur under cyclic compression. *PeerJ,* 4:e1562.

Faith J.T. & Behrensmeyer, A.K. (2006). Changing patterns of carnivore modification in a landscape bone assemblage, Amboseli Park, Kenya. *Journal of Archaeological Science,* 33 (12): 1718-1733.

Faith J.T., Marean, C.W. & Behrensmeyer, A.K. (2007). Carnivore competition, bone destruction and bone

density. *Journal of Archaeological Science,* 34 (12): 2025-2034.

Fernández-Jalvo, Y. (1992). *Tafonomía de Microvertebrados del Complejo Cárstico de Atapuerca (Burgos)*. Universidad Complutense de Madrid, Madrid.

Fernández-Jalvo, Y. & Andrews, P. (2003). Experimental effects of water abrasion on bone fragments. *Journal of Taphonomy*, 1: 147-163.

Fernández-Jalvo, Y. & Andrews, P. (2016). *Atlas of Taphonomic Identifications: 1001+ Images of Fossil and Recent Mammal Bone Modification.* Vertebrate Paleobiology and Paleoanthropology Series, Springer, Dordrecht.

Fiorillo, A.R. (1989). An experimental study of trampling: Implications for the fossil record. In (Bonnichsen, R. & Sorg, M., eds.) *Bone Modification*. Orono: Center for the Study of the First Americans, pp. 61-72.

Fisher, J.W. (1995). Bone surface modification in zooarchaeology. *Journal of Archaeological Method and Theory*, 1: 7-65.

Gifford, D.P. (1981). Taphonomy and paleoecology: a critique review of archaeology's sister disciplines. In (Schiffer, M., ed.) *Advances in Archaeological Method and Theory 4.* New York: Academic Press, pp. 365-438.

González, M., Álvarez, M., Massigoge, A., Gutiérrez, M. & Kaufmann, C.A. (2012). Bone differential survivorship and ontogenic development in guanaco (Lama guanicoe). *International Journal of Osteoarchaeology*, 22: 523-536.

Guadelli, J.L. (2008). La gélifraction des restes fauniques. Expérimentation et transfert au fossile. *Annales de Paléontologie*, 94: 121-165.

Guadelli, J.L. (2015). La gélifraction des restes fauniques. Du laboratoire au terrain. In (Balasse, M., Brugal, J.P., Dauphin, Y., Geigl, E.M., Oberlin, C. & Reiche, I., eds.) *Messages d'Os: Archéométrie du Squelette Animal et Humain.* Editions des Archives Contemporaines, Paris, pp. 177-186.

Guthrie, R.D. (1967). Differential preservation and recovery of Pleistocene large mammal remains in Alaska. *Journal of Paleontology,* 41: 243-246.

Gutiérrez, M.A, González, M., Álvarez, M.C., Massigoge, A. & Kaufmann, C.A. (2016). Meteorización ósea en restos de guanaco y ñandú. *Arqueología,* 22: 57-84.

Ioannidou, E. (2003). Taphonomy of animal bones: species, sex, age and breed: Variability of sheep, cattle and pig bone density. *Journal of Archaeological Science,* 30: 355-365.

Izeta, A.D. (2005). South American camelid bone structural density: what are we measuring? Comments on data sets, values, their interpretation and application. *Journal of Archaeological Science*, 32: 1159-1168.

Janjua, M.A. & Rogers, T.L. (2008). Bone weathering patterns of metatarsal v. femur and the postmortem interval in Southern Ontario. *Forensic Science International*, 178: 16-23.

Junod, C.A. (2013). *Subaerial Bone Weathering and Other Taphonomic Changes in a Temperate Climate.* Boston University School of Medicine, Boston.

Junod, C.A. & Pokines, J.T. (2014). Subaerial weathering. In (Pokines, J.T., & Symes, S.A. eds.) *Manual of Forensic Taphonomy.* Boca Raton: CRC Press, pp. 287-314.

Lam, Y.M., Chen, X. & Pearson, O.M. (1999). Intertaxonomic variability in patterns of bone density and the differential representation of bovid, cervid, and equid elements in the archaeological record. *American Antiquity*, 64: 343-362.

Lyman, R.L. (1994). *Vertebrate Taphonomy*. Cambridge University Press, Cambridge.

Lyman, R.L. & Fox G.L. (1989). A critical evaluation of bone weathering as an indication of bone assemblage formation. *Journal of Archaeological Science*, 16. 293-317.

Madgwick, R. & Mulville, J. (2012). Investigating variation in the prevalence of weathering in faunal assemblages in the UK: a multivariate statistical analysis. *International Journal of Osteoarchaeology*, 22: 509-522.

Marean, C.W. & Kim, S.Y. (1998). Mousterian large mammal remains from Kobeh Cave: behavioral implications for Neanderthals and early modern humans. *Current Anthropology (Supplement),* 39: 79-113.

Massigoge, A., González, M., Kaufmann, C. & Gutiérrez, M.A. (2010). Observaciones actualísticas sobre meteorización ósea en restos esqueletales de guanaco. In (Berón, M., Luna, L., Bonomo, M., Montalvo, C., Aranda, C. & Carrera Aizpitarte, M., eds.) *Mamül Mapu: Pasado y Presente desde la Arqueología Pampeana*. Buenos Aires: Editorial Libros del Espinillo, Tomo 1, pp. 309-322.

Matsuoka, N. (1996). Soil moisture variability in relation to diurnal frost heaving on Japanese high mountain slopes. *Permafrost and Periglacial Processes*, 7: 139-151.

Mengoni Goñalons, G.L. (1999). *Cazadores de Guanacos de la Estepa Patagónica*. Sociedad Argentina de Antropología, Buenos Aires.

Miller, G. J. (1975). A study of cuts, grooves and other marks on recent fossil bone II: weathering cracks, fractures, splinters, and other similar natural phenomena. In (Swanson, E., ed.) *Lithic Technology:*

Making and Using Stone Tools. The Hague: Mouton, pp. 211-226.

Miller, J.H. (2009). *The Large-Mammal Death Assemblage of Yellowstone National Park: Historical Ecology, Conservation Biology, Paleoecology*. University of Chicago, Chicago.

Miotti, L. (1998). *Zooarqueología de la Meseta Central y Costa de la Provincia de Santa Cruz. Un enfoque de las Estrategias Adaptativas Aborígenes y los Paleoambientes*. Museo de Historia Natural, San Rafael.

Pickering, T.R., Marean, C.W. & Domínguez-Rodrigo, M. (2003). Importance of limb bone shaft fragments in Zooarchaeology: a response to "On *in situ* attrition and vertebrate body part profiles" (2002), by M.C. Stiner. *Journal of Archaeological Science,* 30 (11): 1469-1482.

Pokines, J.T. (2009). Forensic recoveries of U.S. war dead and the effects of taphonomy and other site-altering processes. In (Steadman, D.W., ed.) *Hard Evidence: Case Studies in Forensic Anthropology*. Second edition. Upper Saddle River: Prentice Hall, pp. 141-154.

Pokines, J.T., Nowell, A., Bisson, M. S., Cordova, C. E. & Ames, C.J.H. (2011). The functioning of a natural faunal trap in a semi-arid environment: preliminary investigations of WZM-1, a limestone sinkhole site near Wadi Zarqa Ma'in, Hashemite Kingdom of Jordan. *Journal of Taphonomy*, 9: 89-115.

Pokines, J.T., King, R.E., Graham, D.D., Costello. A. K., Adams, D.M., Pendray, J.M., Rao, K. & Siwek, D. (2016). The effects of experimental freeze-thaw cycles to bone as a component of subaerial weathering. *Journal of Archaeological Science: Reports,* 6: 594-602.

Potmesil, M. (2005). Bone dispersion, weathering, and scavenging of cattle bones. *Nebraska Anthropologist. Paper* 6: 26-32. http://digitalcommons.unl.edu/nebanthro/6 (Accessed 5 may 2017).

Riggs, C.M., Lanyon, L.E. & Boyde, A. (1993). Functional associations between collagen fibre orientation and locomotor strain direction in cortical bone of the equine radius. *Anatomy and Embryology,* 187 (3): 231-238.

Rindel, D. & Bourlot, T. (2014). Zooarqueología de la cuenca del Lago Cardiel. In (Goñi, R, Belardi, J. B., Cassiodoro, G. & Re, A., eds.) *Arqueología de las Cuencas de los Lagos Cardiel y Strobel. Poblamiento Humano y Paleoambientes en Patagonia*. Buenos Aires: Aspha Ediciones, pp. 97-115.

Stahl, P.W. (1999). Structural density of domesticated South American Camelid skeletal element and the archaeological investigation of prehistoric Andean ch´arki. *Journal of Archaeological Science,* 26 (11): 1347-1368.

Steele, D.G. & Carson, D.L. (1989). Excavation and taphonomy of mammoth remains from the Duewall-Newberry Site, Brazos County, Texas. In (Bonnischen, R. & Sorg, M.H., eds.) *Bone Modification*. Orono: Center for the Study of the First Americans, pp. 413-430.

Tappen, M. (1994). Bone weathering in the tropical rain forest. *Journal of Archaeological Science,* 21: 667-673.

Todd, L.C., Witter, R.V. & Frison, G.C. (1987). Excavation and documentation of the Princeton and Smithsonian Horner Site assemblages. In (G.C. Frison & Todd, L.C., eds.) *The Horner Site: the Type Site of the Cody Cultural Complex*. Orlando: Academic Press, pp. 39-91.

Ubelaker, D.H. & Sperber, N.D. (1988). Alterations in human bones and teeth as a result of restricted sun exposure and contact with corrosive agents. *Journal of Forensic Sciences,* 33: 540-548.

Yravedra, J. & Domínguez-Rodrigo, M. (2009). The shaft-based methodological approach to the quantification of long limb bones and its relevance to understanding hominid subsistence in the Pleistocene: application to four Paleolithic sites. *Journal of Quaternary Science,* 24 (1): 85-96.